

ВЛИЯНИЕ МЕХАНИЧЕСКОЙ АКТИВАЦИИ РЕАГЕНТОВ НА СИНТЕЗ Li-Sm ФЕРРИТА**Е.Н. Лысенко, А.П. Суржиков, В.А. Власов, Е.В. Николаев, Ю.С. Минина, Е.А. Шевелева**

Елена Николаевна Лысенко (ORCID 0000-0002-5093-2207)*, Анатолий Петрович Суржиков (ORCID 0000-0003-2795-398X), Виталий Анатольевич Власов (ORCID 0000-0002-5946-2117), Евгений Владимирович Николаев (ORCID 0000-0002-2663-3207), Юлия Сергеевна Минина (ORCID 0000-0002-2708-9872)

Проблемная научно-исследовательская лаборатория электроники, диэлектриков и полупроводников, Исследовательская школа физики высокогенергетических процессов, Национальный исследовательский Томский политехнический университет, пр. Ленина, 30, Томск, Российская Федерация, 634034

E-mail: lysenkoen@tpu.ru*, surzhikov@tpu.ru, vlvitan@tpu.ru, nikolaev0712@tpu.ru, ysm7@tpu.ru

Елена Александровна Шевелева (ORCID 0000-0002-6013-5519)

Отделение контроля и диагностики, Инженерная школа неразрушающего контроля и безопасности, Национальный исследовательский Томский политехнический университет, пр. Ленина, 30, Томск, Российская Федерация, 634034

E-mail: vasendina@tpu.ru

Методами рентгенофазового анализа, термогравиметрии и дифференциально-сканирующей калориметрии проведены исследования влияния энергонапряженности механического измельчения смеси порошковых реагентов Sm_2O_3 (14,7вес. %)/ Fe_2O_3 (77,5вес. %)/ Li_2CO_2 (7,8вес. %) на процесс синтеза Li-Sm феррита. В работе использовалась шаровая мельница Retsch E-max, обеспечивающая разную энергонапряженность механического измельчения путем варьирования скорости вращения стаканов 300, 1000, 1500 об/мин. Реакцию взаимодействия между исходными реагентами изучали путем нагрева порошковой смеси на воздухе до 900 °C в печи термического анализатора Netzsch STA 449C Jupiter. Полный цикл синтеза феррита, включающий изотермическую выдержку при высокой температуре, был проведен в лабораторной печи при температуре 900 °C в течение 240 мин. Установлено, что с увеличением энергонапряженности измельчения порошков температурный интервал взаимодействия между $Sm_2O_3/Fe_2O_3/Li_2CO_3$ сдвигается на 200 °C в область меньших температур, что указывает на увеличение реакционной способности порошковых реагентов. При этом в процессе синтеза образуется двухфазный композиционный материал, состоящий из незамещенного литиевого феррита $\alpha-Li_{0,5}Fe_{2,5}O_4$ (81,0-81,8 вес. %) и $SmFeO_3$ (18,2-19 вес. %). Концентрационное соотношение синтезированных фаз в пределах экспериментальной ошибки не зависит от энергонапряженности измельчения исходных реагентов. Синтезирование незамещенного литиевого феррита было подтверждено данными рентгенофазового анализа (параметр решетки ~0,833 нм), наличием эндотермического пика на дифференциально-термической кривой, соответствующего переходу $\alpha-Li_{0,5}Fe_{2,5}O_4 \rightarrow \beta-Li_{0,5}Fe_{2,5}O_4$, а также значением температуры Кюри (~630 °C), полученным методом термогравиметрии в магнитном поле. Полученный результат может быть полезен при разработке технологии получения новых композиций ферритов с редкоземельными элементами, обладающими уникальными свойствами.

Ключевые слова: литий-самариевый феррит, редкоземельный элемент, Sm_2O_3 , механическая активация, синтез, термический анализ

EFFECT OF MECHANICAL ACTIVATION OF REAGENTS ON SYNTHESIS OF Li-Sm FERRITE

E.N. Lysenko, A.P. Surzhikov, V.A. Vlasov, E.V. Nikolaev, Yu.S. Minina, E.A. Sheveleva

Elena N. Lysenko (ORCID 0000-0002-5093-2207)*, Anatoliy P. Surzhikov (ORCID 0000-0003-2795-398X), Vitaliy A. Vlasov (ORCID 0000-0002-5946-2117), Evgeniy V. Nikolaev (ORCID 0000-0002-2663-3207), Yuliya S. Minina (ORCID 0000-0002-2708-9872)

Research Laboratory of Electronics, Semiconductors and Dielectrics, Research School of High-Energy Physics, National Research Tomsk Polytechnic University, Lenina ave., 30, Tomsk, 634034, Russia
E-mail: lysenko@tpu.ru*, surzhikov@tpu.ru, vlvitan@tpu.ru, nikolaev0712@tpu.ru, ysm7@tpu.ru

Elena A. Sheveleva

Division for Testing and Diagnostics, School of Non-Destructive Testing, National Research Tomsk Polytechnic University, Lenina ave., 30, Tomsk, 634034, Russia
E-mail: vasendina@tpu.ru

The effect of the energy intensity of mechanical grinding of Sm_2O_3 (14.7 wt.%)/ Fe_2O_3 (77.5 wt.%)/ Li_2CO_3 (7.8 wt.%) powder reagents on synthesis of Li-Sm ferrite was investigated by X-ray diffraction analysis, thermogravimetry, and differential scanning calorimetry. The study used a Retsch E-max ball mill, which provides different energy intensity of mechanical grinding at different rotational speed of 300, 1000, and 1500 rpm. The interaction between the initial reagents was analyzed through heating the powder mixture to 900 °C in air in the furnace of the Netzsch STA 449C Jupiter thermal analyzer. A complete cycle of ferrite synthesis, including high temperature isothermal holding, was performed in the laboratory furnace at 900 °C for 240 min. It was found that at increased energy intensity of powder grinding, the temperature range of interaction between $\text{Sm}_2\text{O}_3/\text{Fe}_2\text{O}_3/\text{Li}_2\text{CO}_3$ shifts to lower temperatures by 200 °C, which indicates an increased reactivity of powder reagents. In this case, a two-phase composite material is formed during synthesis, which consists of unsubstituted lithium ferrite $\alpha\text{-Li}_{0.5}\text{Fe}_{2.5}\text{O}_4$ (81.0–81.8 wt.%) and SmFeO_3 (18.2–19 wt.%). Within the limits of the experimental error, the concentration ratio of the synthesized phases does not depend on the energy intensity of grinding the initial reagents. Synthesis of unsubstituted lithium ferrite was confirmed by X-ray diffraction data (lattice parameter of ~0.833 nm), an endothermic peak in the differential scanning curve indicating the $\alpha\text{-Li}_{0.5}\text{Fe}_{2.5}\text{O}_4 \rightarrow \beta\text{-Li}_{0.5}\text{Fe}_{2.5}\text{O}_4$ transition, and by the Curie temperature (~630 °C) determined by thermogravimetry in a magnetic field. The result obtained may generate interest in the technology of ferrites of new compositions substituted with rare earth elements, which possess unique properties.

Key words: lithium-samarium ferrite, rare earth element, Sm_2O_3 , mechanical activation, synthesis, thermal analysis

Для цитирования:

Лысенко Е.Н., Суржиков А.П., Власов В.А., Николаев Е.В., Минина Ю.С., Шевелева Е.А. Влияние механической активации реагентов на синтез Li-Sm феррита. *Изв. вузов. Химия и хим. технология*. 2024. Т. 67. Вып. 3. С. 63–72. DOI: 10.6060/ivkkt.20246703.6931.

For citation:

Lysenko E.N., Surzhikov A.P., Vlasov V.A., Nikolaev E.V., Minina Yu.S., Sheveleva E.A. Effect of mechanical activation of reagents on synthesis of Li-Sm ferrite. *ChemChemTech [Izv. Vyssh. Uchebn. Zaved. Khim. Khim. Tekhnol.]*. 2024. V. 67. N 3. P. 63–72. DOI: 10.6060/ivkkt.20246703.6931.

INTRODUCTION

The operational properties of ferrites directly depend on their phase composition and the microstructure formed during their synthesis and sintering [1-2]. Unsubstituted lithium ferrite with the chemical formula $\text{Li}_{0.5}\text{Fe}_{2.5}\text{O}_4$ (LiFe_5O_8) has a high Curie point (~630 °C) and a high saturation magnetization value,

which potentiates its application for cores of transformers, antennas, and magnetic recorders [3-6]. Lithium ferrites used in microwave technology typically exhibit a complex composition attained by replacing iron ions, for example, with nickel, magnesium, titanium, zinc, and manganese ions [7-9]. These substitutions enabled production of ferrites with a specific combination of electrical and magnetic properties.

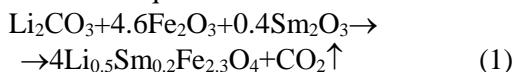
Lithium ferrites of new compositions possessing unique properties remain to be of compelling interest today.

The studies conducted in recent years have been focused on properties of different ferrites substituted with rare earth elements (REE). As shown in [10-14], incorporation of rare earth elements, including samarium, significantly affects electromagnetic properties of various ferrites. In most of the studies, synthesis of ferrites with REE and their microstructural characteristics were studied by X-ray diffraction analysis (XRD). It was suggested that the formation of substituted ferrites with a small inclusion of secondary phases (for example, GdFeO_3 and SmFeO_3 , depending on the incorporated REE) affects the properties of the synthesized ferrites [15, 16]. In many cases, the basic method of ferrite production is ceramic technology, which uses oxides and carbonates as initial reagents [17-21].

In [22], we showed that no substituted phase of lithium ferrite was formed during the interaction of $\text{Sm}_2\text{O}_3/\text{Fe}_2\text{O}_3/\text{Li}_2\text{CO}_3$ reagents taken in different weight ratios. Ball milling of the initial oxides is known not only to change the system dispersity, but also to increase the activity of the powders, which essentially affects the course of the solid-phase reaction between the initial reagents [23-26]. The results obtained in [27-28] show that grinding of powder systems (for example, $\text{Fe}_2\text{O}_3/\text{Li}_2\text{CO}_3$, $\text{Fe}_2\text{O}_3/\text{Li}_2\text{CO}_3/\text{ZnO}$, $\text{Fe}_2\text{O}_3/\text{Li}_2\text{CO}_3/\text{TiO}_2$) in a planetary mill accelerates synthesis of substituted lithium ferrites and reduces the temperature of their synthesis. In this regard, we can suggest that high-energy pre-grinding of the initial reagents changes the phase formation of REE substituted ferrites. Thus, the aim of this study was to analyze the effect of the energy intensity of grinding the initial reagents $\text{Sm}_2\text{O}_3/\text{Fe}_2\text{O}_3/\text{Li}_2\text{CO}_3$ on synthesis of lithium-samarium ferrite.

EXPERIMENTAL

The initial reagents used for lithium ferrite synthesis were lithium carbonate Li_2CO_3 (chemically pure), iron oxide Fe_2O_3 (analytically pure), and samarium oxide Sm_2O_3 ($\text{REO} > 99.99\%$). The ratio of the initial components in the reaction mixture $\text{Sm}_2\text{O}_3/\text{Fe}_2\text{O}_3/\text{Li}_2\text{CO}_3$ (14.7/77.5/7.8 wt.%) was calculated by the chemical equation:



The $\text{Sm}_2\text{O}_3/\text{Fe}_2\text{O}_3/\text{Li}_2\text{CO}_3$ powder mixture (10 g per jar) was ground in a Retsch E-max high-speed ball mill using 5 mm stainless-steel balls and 125 ml jars at a rotational speed of 300, 1000, and 1500 rpm. The grinding time was 30 min. The powder to ball ratio was 1:10. It is known that efficient grinding in the specified

ball mill is achieved through high-frequency impact, intense friction and controlled circular movements of the grinding bowl [29]. The adaption of the kinematic model from a planetary ball mill to the high-energy Retsch E-max mill was detailed in [30]. Thus, energy dose (E) that generated by mechanical milling process on the powder can be calculated according to Eq. (2) [30]:

$$E = \varphi_b N_b m_b t \omega_p^3 (R_j - \frac{d_b}{2} + R_p) \frac{(R_j - \frac{d_b}{2})}{\pi} \quad (2)$$

where N_b , m_b , ω_p , R_j , R_p and d_b refer to total ball count, mass of ball (kg), rotational speed (rad/s), jar radius ($1.68 \cdot 10^{-2}$ m for the 125 ml jar), distance between the center of the plate and the center of the jar ($1.6 \cdot 10^{-2}$ m) and ball diameter (m), respectively. The parameter φ_b is the yield coefficient that provides the energy dissipated by the impact of one ball against the grinding jar wall in a system with multiple balls. Its value depends on the ratio of total ball count to the maximum ball count that can be contained in the jar and is analytically found to be equal to 0.95. The energy dose transferred to the particles with the reference to mechanical milling duration was calculated as 0.7, 27.1 and 91.4 kJ for the rotational speed of 300, 1000, and 1500 rpm, respectively.

The interaction reaction between the initial reagents was studied by the thermogravimetric (TG) analysis and differential calorimetry (DSC) using the Netzsch STA 449C Jupiter thermal analyzer. For this, sample with a mass of ca. 10 mg was placed in an alumina crucible and heated up to 900 °C in air at a heating rate of 10 °C/min, followed by cooling at a rate of 20 °C/min.

Ferrite samples were synthesized at 900 °C for 240 min in air in the laboratory furnace.

The magnetic ferrite phase additionally formed during synthesis was studied by TG analysis with the application of an external magnetic field as described in [31]. For this, the two permanent magnets were attached on the outer side of the measurement cell so that the sample is located in a magnetic field of ca. 5 Oe. The heating rate during thermomagnetometric analysis was 50 °C/min, which was the maximum for this device. The Netzsch Proteus software packages were used for data analysis.

XRD analysis of the samples was performed using an ARL X'TRA diffractometer with a Peltier Si(Li) semiconductor detector and CuK_α radiation (37 kV voltage and 35 mA current). The X-ray diffraction (XRD) patterns were measured for $2\theta = (10-90)^\circ$ with a scan rate of 0.02 °/s and scanning speed 1.2 °/min. The phases were identified using the PDF-4+ powder database of the International Center for Diffraction Data (ICDD). PowderCell 2.4 software was used to

quantify phases (full-profile analysis), crystallite sizes by the Williamson-Hall method and verify the lattice parameters. The full-profile method is so-called standardless quantitative XRD analysis using by Pseudo-Voight function.

RESULTS AND DISCUSSION

The data obtained by thermal analysis of the $\text{Sm}_2\text{O}_3/\text{Fe}_2\text{O}_3/\text{Li}_2\text{CO}_3$ powder mixture, mechanically activated under different modes, are shown in Fig. 1.

The TG curve of the powders heated in the thermal analyzer (Fig. 1 (a–c)) shows several stage decrease in their weight. A slight decrease in the weight of the samples heated up to 200 °C is related to the removal of moisture physically adsorbed during grinding and storage of powders. As previously shown in [22], the decrease in weight in the temperature range of 280–450 °C is due to weight changes in Sm_2O_3 . At increased energy intensity of grinding, the weight loss increases from 0.99% (Fig. 1 (a)) to 1.52% (Fig. 1 (c)); yet it is insignificant and, according to [32], this process is related to the loss of physically and chemically adsorbed water, which is accompanied by endothermic thermal effects, as seen in the DSC curve.

Further temperature increase significantly changes the sample weight due to the release of CO_2 during the diffusion interaction between the $\text{Sm}_2\text{O}_3/\text{Fe}_2\text{O}_3/\text{Li}_2\text{CO}_3$ reagents, as evidenced by Eq. (1). The temperature range of this interaction shifts to lower temperatures at increased energy intensity of grinding. Thus, the start of the ferrite synthesis reaction decreases from 500 °C for powders pre-activated at 300 rpm to 350 °C for powders ground at a rotational speed of 1500 rpm. The final temperature of interaction between the reagents with the release of CO_2 also decreases from 700 to 520 °C, respectively.

Thus, mechanical activation of the reagent mixture accelerates the synthesis reaction between the $\text{Sm}_2\text{O}_3/\text{Fe}_2\text{O}_3/\text{Li}_2\text{CO}_3$ reagents. The total weight loss in this temperature range varies slightly for different samples (4.59–4.87 %), but these values are close to the value of 4.64 % for CO_2 release calculated by Eq. (1). The interaction between the reagents in all the studied samples proceeds in two stages, which is related to melting and decomposition of lithium carbonate, the element of the powder mixture.

It is known [22] that decomposition of pure lithium carbonate according to the scheme



starts at a temperature near its melting point, which varies within 720–735 °C (according to reference data). Its decomposition accelerates when lithium carbonate is mixed with metal oxides. In particular, when Li_2CO_3

is mixed with Fe_2O_3 , its accelerated decomposition is attributed to the predominant diffusion of Fe^{3+} cations into the crystal lattice of Li_2CO_3 . Therefore, the thermal analysis data obtained in this study show a lower temperature of Li_2CO_3 decomposition in the $\text{Sm}_2\text{O}_3/\text{Fe}_2\text{O}_3/\text{Li}_2\text{CO}_3$ mixture.

The results of studies [27, 33] on the influence of the chemical and thermal pre-history of the Fe_2O_3 reagent on its interaction with Li_2CO_3 to produce lithium ferrites showed that the reaction is limited mainly by diffusion interactions at 500 °C and above. However, during this interaction, the initial reaction product formed at low temperatures is lithium ferrite LiFeO_2 , regardless of the ratio of the initial components. At the initial molar ratio of Li_2CO_3 to Fe_2O_3 of 1:5 and at increased synthesis temperature and duration, the reaction product formed is lithium ferrite $\text{Li}_{0.5}\text{Fe}_{2.5}\text{O}_4$.

In this regard, a two-step change in the sample weight in the TG curve and the corresponding double peak in the DSC curve observed in all the studied samples is due to the formation of transitional phases of lithium ferrite. This is evidenced by an insignificant peak recorded in the DSC curve at ~ 750 °C (Fig. 1 (a–c)), which is related to the order-disorder phase transition ($\alpha \rightarrow \beta$) in the resulting $\text{Li}_{0.5}\text{Fe}_{2.5}\text{O}_4$ phase [27].

A reverse $\beta \rightarrow \alpha$ transition of higher intensity caused by additional heating, at which further synthesis occurs, can be observed in the DSC curve obtained during cooling (Fig. 1 (d–f)). As reported in [34], transition of the $\alpha\text{-Li}_{0.5}\text{Fe}_{2.5}\text{O}_4$ phase to the $\beta\text{-Li}_{0.5}\text{Fe}_{2.5}\text{O}_4$ phase in pure lithium ferrite causes a DSC peak of 12 J/g. Fig. 1 (d–f) shows that the enthalpy transition values for the samples attain 6.4–8.1 J/g, which corresponds to partial formation of the lithium ferrite phase.

Fig. 1 (d–f) also presents the results of the thermomagnetometric analysis when the magnets were attached once the sample heating was completed in accordance with the scheme presented in [31]. The TG curves measured in the magnetic field show a weight jump, which is related not to the changed sample weight, but to the interaction of the synthesized magnetic phase with the external magnetic field applied. This weight jump, the height of which indicates sample magnetization, occurs near the Curie point (T_c) that can be determined based on the derivative thermogravimetric (DTG) curve. The Curie point for weakly activated (at 300 rpm) samples attains 629.7 °C, and these values are close to the magnetic transition temperature in lithium ferrite at $T_c = 620\text{--}632$ °C, depending on the literature source [35–37]. As reported in [34, 38], a slight decrease in the Curie temperature in samples mechanically pre-ground at 1000 and 1500 rpm can be due to the increased disorder in the ferrite structure,

that is, due to partially formed β -Li_{0.5}Fe_{2.5}O₄ phases. This is confirmed by the decreased area of the DSC peak in mechanically activated samples, which corresponds to the $\beta \rightarrow \alpha$ transition during cooling. However, this should not decrease sample magnetization, which

is evidenced by the decreased weight jump in the activated samples. Therefore, we can assume the formation of a certain amount of a weakly substituted phase of lithium ferrite due to the interaction of reagents with samarium oxide that decreases the Curie temperature of the magnetic phase.

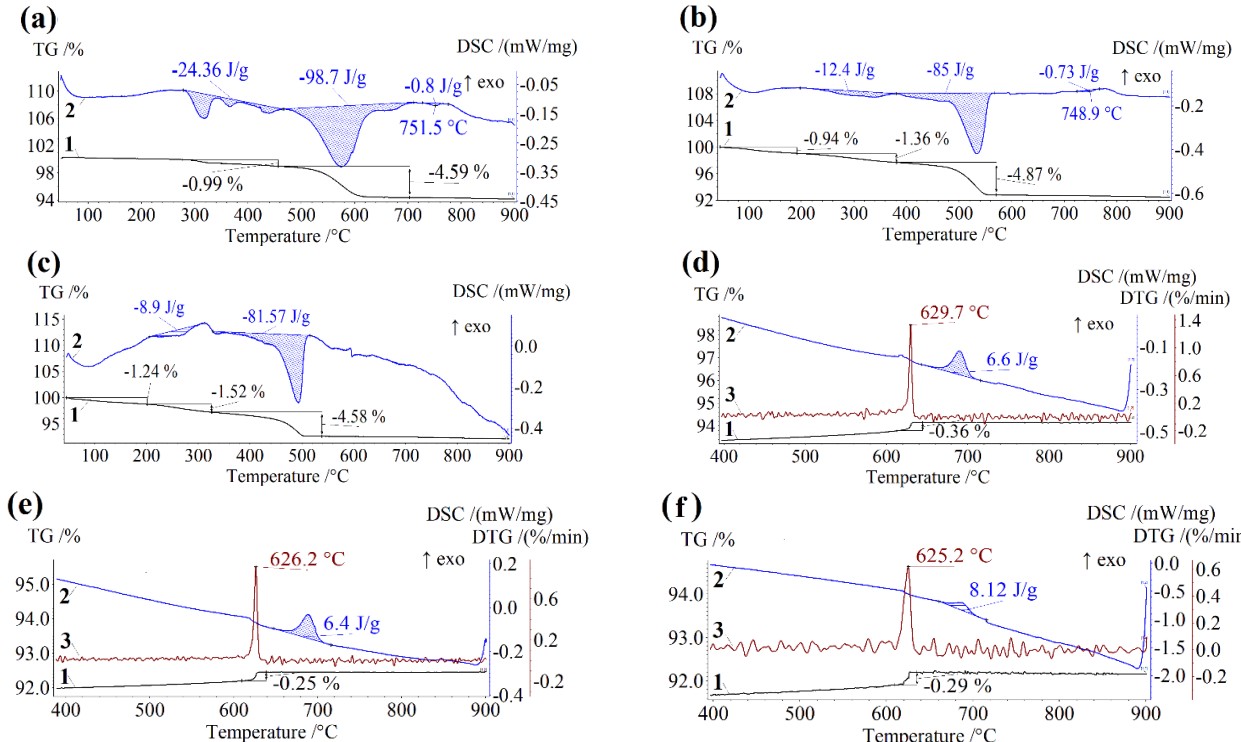


Fig. 1. TG (curves 1), DSC (curves 2) analysis upon heating (a-c) and thermomagnetometric (curves 3) analysis upon cooling (d-f) of Sm₂O₃/Fe₂O₃/Li₂CO₃ mixture mechanically pre-activated under 300 (a, d), 1000 (b, e), and 1500 (c, f) rpm

Рис. 1. ТГ (кривые 1), ДСК (кривые 2) анализ при нагреве (а-с) и терромагнитометрический (кривые 3) анализ при охлаждении (д-ф) смеси исходных реагентов Sm₂O₃/Fe₂O₃/Li₂CO₃, предварительно механоактивированной при 300 (а, д), 1000 (б, е) и 1500 (с, ф) об/мин

Fig. 2 presents the results of the thermal analysis of the samples synthesized at 900 °C for 240 min from mechanically activated powders. DSC analysis revealed high values of the enthalpy of transition from α -Li_{0.5}Fe_{2.5}O₄ to β -Li_{0.5}Fe_{2.5}O₄ phase, which shows that the synthesized samples contain mainly lithium ferrite in their composition.

The content of α -Li_{0.5}Fe_{2.5}O₄ slightly decreases at increased energy intensity of grinding of the initial reagents, which is evidenced by the patterns obtained for the decreased enthalpy of the DSC peak and the Curie temperature. Thus, the obtained results indicate the formation of a significant amount of unsubstituted lithium ferrite with the chemical formula Li_{0.5}Fe_{2.5}O₄ during solid-phase interaction in the Sm₂O₃/Fe₂O₃/Li₂CO₃ mixture. The enthalpy values of the transition of α -Li_{0.5}Fe_{2.5}O₄ to β -Li_{0.5}Fe_{2.5}O₄ obtained by DSC analysis, and the weight jump values in the magnetic field obtained by TG analysis can be used to estimate the content of lithium ferrite in the total

powder; it exceeds 50 wt.% at the stage of mixture cooling in the thermal analyzer.

For comprehensive analysis of the ferrite synthesis processes, we performed XRD analysis of the samples synthesized at 900 °C for 240 min. Fig. 3 shows XRD patterns for samples mechanically activated under different modes. Table 1 summarizes the XRD data obtained.

It was found that part of the resulting reflections belong to the cubic spinel space group *Fd-3m*. According to the data on the lattice parameter of ~ 8.33 Å, this phase belongs to unsubstituted lithium ferrite. The presence of reflections at $2\theta \approx 15^\circ$, 23° and 26° indicates the formation of the ordered phase α -Li_{0.5}Fe_{2.5}O₄ (PDF No. 04-015-5965), with three Fe³⁺ ions and one L⁺ ion located in octahedral positions along the crystallographic directions <110>. The data presented in the table show that the lattice parameter of the synthesized lithium ferrite decreases, whereas the crystallite size grows at increased grinding energy.

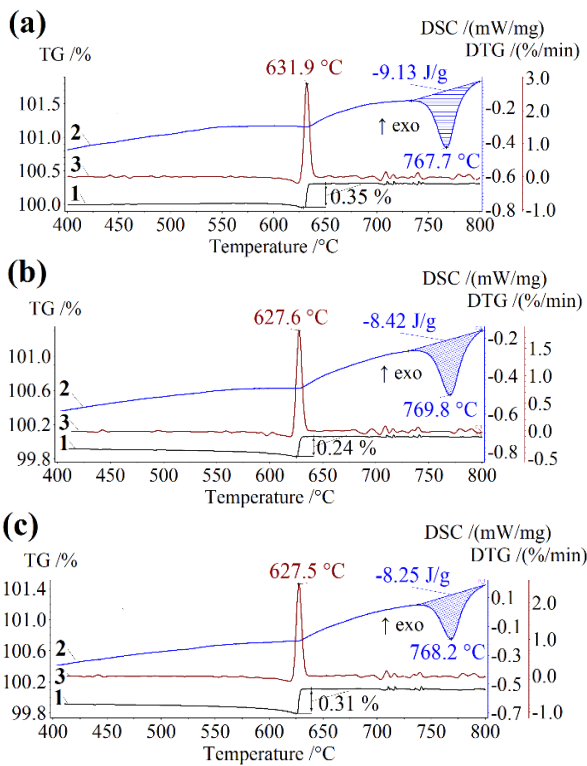


Fig. 2. TG (curves 1), DSC (curves 2) and thermomagnetometric (curves 3) analysis obtained during heating of ferrite samples pre-activated under 300 (a), 1000 (b) and 1500 (c) rpm and synthesized at 900 °C for 240 min

Рис. 2. ТГ (кривые 1), ДСК (кривые 2) и термомагнитометрический (кривые 3) анализ, выполненный при нагреве ферритовых образцов, предварительно активированных при 300 (а), 1000 (б) и 1500 (с) об/мин и синтезированных при 900 °C в течение 240 мин

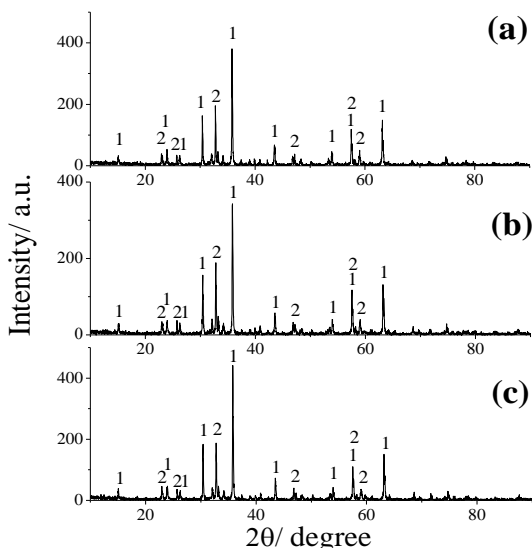


Fig. 3. XRD analysis of ferrite samples pre-activated under 300 (a), 1000 (b) and 1500 (c) rpm and synthesized at 900 °C for 240 min
(1 - Li_{0.5}Fe_{2.5}O₄; 2 - SmFeO₃)

Рис. 3. Рентгенофазовый анализ ферритовых образцов, предварительно активированных при 300 (а), 1000 (б) и 1500 (с) об/мин и синтезированных при 900 °C в течение 240 мин
(1 - Li_{0.5}Fe_{2.5}O₄; 2 - SmFeO₃)

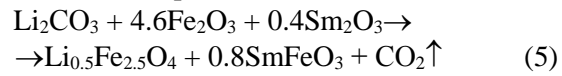
Along with lithium ferrite, a secondary crystalline phase is formed in the amount of 18-19 wt.%, identified as SmFeO₃ (PDF No. 00-039-1490). As reported in [15, 16], the formation of this phase was previously observed during synthesis of ferrites of other compositions. It should be noted that SmFeO₃ is a non-magnetic material with an orthorhombic space group (*Pnma*). Formation of this phase can be initiated by the reaction



Table
XRD data of synthesized ferrite samples
Таблица. РФА данные синтезированных ферритовых образцов

Grinding mode	Phase	Lattice parameter	Crystallite size	Phase concentration
rpm		Å	nm	wt.%
300	Li _{0.5} Fe _{2.5} O ₄	a=b=c=8.3307	99	81.8
	SmFeO ₃	a=5.5936; b=7.7046; c=5.3995	101	18.2
1000	Li _{0.5} Fe _{2.5} O ₄	a=b=c=8.3281	124	81.0
	SmFeO ₃	a=5.5869; b=7.7087; c=5.4013	176	19.0
1500	Li _{0.5} Fe _{2.5} O ₄	a=b=c=8.3269	151	81.5
	SmFeO ₃	a=5.5850; b=7.7063; c=5.3992	132	18.5

The XRD data show the formation of a two-phase product based on Li_{0.5}Fe_{2.5}O₄ and SmFeO₃ during solid-phase interaction; its quantitative content is indicated in Table. With regard to the above, the solid-phase interaction between the initial reagents Sm₂O₃/Fe₂O₃/Li₂CO₃ proceeds as follows:



XRD and thermal analyses show that the substituted lithium ferrite is not formed during interaction of the above initial reagents, regardless of the energy intensity of their mechanical grinding. In this case, a two-phase composite material Li_{0.5}Fe_{2.5}O₄-SmFeO₃ is synthesized.

CONCLUSION

Mechanical activation of the mixture of initial reagents Sm₂O₃/Fe₂O₃/Li₂CO₃ in a ball mill has an effect on ferrite synthesis. At increased energy intensity of grinding of the initial powders that depends on the milling rotational speed, the initial and final temperatures of the interaction between Sm₂O₃/Fe₂O₃/Li₂CO₃

with CO₂ release shift to lower temperatures, indicating an increased powder reactivity. In this case, regardless of the energy intensity of grinding, heating of the Sm₂O₃/Fe₂O₃/Li₂CO₃ mixture results in the formation of a two-phase product, which consists mainly of the ordered phase of lithium ferrite α -Li_{0.5}Fe_{2.5}O₄ and the SmFeO₃ phase. Thus, mechanical activation of the initial powders did not have the desired effect on the production of samarium substituted lithium ferrite, which is to some extent not consistent with the literature data reported for the production of REE substituted ferrites. Despite this, the obtained result is of high relevance for production of lithium-containing ferrites of new compositions substituted with rare earth elements that possess unique properties. It can be assumed that the formation of the two-phase composite material Li_{0.5}Fe_{2.5}O₄-SmFeO₃ can primarily affect the electrical

properties of ferrites. In this regard, the electrical and magnetic properties of the synthesized ferrites should be further studied.

The work was supported by the Ministry of Science and Higher Education of the Russian Federation as part of the state task in the field of scientific activity (project FSWW-2023-0011).

The authors declare the absence a conflict of interest warranting disclosure in this article.

Работа выполнена при финансовой поддержке Министерства науки и высшего образования Российской Федерации в рамках государственного задания в сфере научной деятельности (проект FSWW-2023-0011).

Авторы заявляют об отсутствии конфликта интересов, требующего раскрытия в данной статье.

ЛИТЕРАТУРА

- Григорьева И.О., Дресвянников А.Ф. Электрохимический синтез дисперсного феррита бария с использованием анодного растворения металла. *Изв. вузов. Химия и хим. технология.* 2021. Т. 64. Вып. 4. С. 59-66. DOI: 10.6060/ivkkt.20216404.6315.
- Шабельская Н.П., Сулима С.И., Сулима Е.В., Власенко А.И. Изучение особенностей синтеза наноразмерного феррита цинка. *Изв. вузов. Химия и хим. технология.* 2016. Т. 59. Вып. 1. С. 39-42. DOI: 10.6060/tctc.20165901.5223.
- Mazen S.A., Abu-Elsaad N.I. Structural, magnetic and electrical properties of the lithium ferrite obtained by ball milling and heat treatment. *Appl. Nanosci.* 2015. V. 5. P. 105-114. DOI: 10.1007/s13204-014-0297-2.
- Ahmad M., Shahid M., Alanazi Y.M., Rehman A.U., Asif M., Dunnill C.W. Lithium ferrite (Li_{0.5}Fe_{2.5}O₄): synthesis, structural, morphological and magnetic evaluation for storage devices. *J. Mater. Res. Technol.* 2022. V. 18. P. 3386-3395. DOI: 10.1016/j.jmrt.2022.03.113.
- Granados-Miralles C., Serrano A., Prieto P., Guzmán-Mínguez J., Prieto J.E., Friedel A.M., García-Martín E., Fernández J.F., Quesada A. Quantifying Li-content for compositional tailoring of lithium ferrite ceramics. *J. Eur. Ceram. Soc.* 2023. V. 43. P. 3351-3359. DOI: 10.1016/j.jeurceramsoc.2023.02.011.
- Teixeira S.S., Graça M.P.F., Costa L.C. Dielectric, morphological and structural properties of lithium ferrite powders prepared by solid state method. *J. Non-Cryst. Solids.* 2012. V. 358. P. 1924-1929. DOI: 10.1016/j.jnoncrysol.2012.06.003.
- Исаев И.М., Костишин В.Г., Шакирзянов Р.И., Каюмова А.Р., Салогуб Д.В. Электромагнитные свойства полимерных композитов Li_{0.33}Fe_{2.29}Zn_{0.21}Mn_{0.17}O₄/П(ВДФ-ТФЭ) в области частот 100-7000 МГц. *Физика и техника полупроводников.* 2022. № 1. С. 114-119. DOI: 10.21883/FTP.2022.01.51821.9728.

REFERENCES

- Grigoryeva I.O., Dresvyanikov A.F. Electrochemical synthesis of dispersed barium ferrite using anodic dissolution of metal. *ChemChemTech [Izv.Vyssh. Uchebn. Zaved. Khim. Khim. Tekhnol.J.* 2021. V. 64. N 4. P. 59-66 (in Russian). DOI: 10.6060/ivkkt.20216404.6315.
- Shabelskaya N., Sulima S., Sulima E., Vlasenko A. Study of the features of the synthesis of nanosized zinc ferrite. *ChemChemTech [Izv. Vyssh. Uchebn. Zaved. Khim. Khim. Tekhnol.J.* 2016. V. 59. N 1. P. 39-42 (in Russian). DOI: 10.6060/tctc.20165901.5223.
- Mazen S.A., Abu-Elsaad N.I. Structural, magnetic and electrical properties of the lithium ferrite obtained by ball milling and heat treatment. *Appl. Nanosci.* 2015. V. 5. P. 105-114. DOI: 10.1007/s13204-014-0297-2.
- Ahmad M., Shahid M., Alanazi Y.M., Rehman A.U., Asif M., Dunnill C.W. Lithium ferrite (Li_{0.5}Fe_{2.5}O₄): synthesis, structural, morphological and magnetic evaluation for storage devices. *J. Mater. Res. Technol.* 2022. V. 18. P. 3386-3395. DOI: 10.1016/j.jmrt.2022.03.113.
- Granados-Miralles C., Serrano A., Prieto P., Guzmán-Mínguez J., Prieto J.E., Friedel A.M., García-Martín E., Fernández J.F., Quesada A. Quantifying Li-content for compositional tailoring of lithium ferrite ceramics. *J. Eur. Ceram. Soc.* 2023. V. 43. P. 3351-3359. DOI: 10.1016/j.jeurceramsoc.2023.02.011.
- Teixeira S.S., Graça M.P.F., Costa L.C. Dielectric, morphological and structural properties of lithium ferrite powders prepared by solid state method. *J. Non-Cryst. Solids.* 2012. V. 358. P. 1924-1929. DOI: 10.1016/j.jnoncrysol.2012.06.003.
- Isaev I.M., Kostishin V.G., Shakirzyanov R.I., Kayumova A.R., Salogub D.V. Electromagnetic properties of polymer composites Li_{0.33}Fe_{2.29}Zn_{0.21}Mn_{0.17}O₄/P(VDF-TFE) in the frequency range 100 MHz - 7000 MHz. *Fizika Tehnika Poluprovodnikov.* 2022. V. 56. N 1. P. 114-119 (in Russian). DOI: 10.21883/FTP.2022.01.51821.9728.

8. Isaev I.M., Kostishin V.G., Korovushkin V.V., Shipko M.N., Timofeev A.V., Mironovich A.Yu., Salogub D.V., Shakirzyanov R.I. Кристаллохимия и магнитные свойства поликристаллических ферритов-спинелей $\text{Li}_{0.33}\text{Fe}_{2.29}\text{Zn}_{0.21}\text{Mn}_{0.17}\text{O}_4$. Журн. неорг. химии. 2021. Т. 66. № 12. Р. 1792-1800. DOI: 10.31857/S0044457X21120059.
9. Isaev I.M., Kostishin V.G., Korovushkin V.V., Salogub D.V., Shakirzyanov R.I., Timofeev A.V., Mironovich A.Yu. Магнитные и радиопоглощающие свойства поликристаллического феррита-спинели $\text{Li}_{0.33}\text{Fe}_{2.29}\text{Zn}_{0.21}\text{Mn}_{0.17}\text{O}_4$. Журн. техн. физики. 2021. Т. 91. № 9. Р. 1376-1380. DOI: 10.21883/JTF.2021.09.51217.74-21.
10. AsifIqbal M., Islam M.U., Ali I., Khan M.A., Sadiq I., Ali I. High frequency dielectric properties of Eu+3-substituted Li-Mg ferrites synthesized by sol-gel auto-combustion method. *J. Alloys Compd.* 2014. V. 586. P. 404-410. DOI: 10.1016/j.jallcom.2013.10.066.
11. Zhong X.C., Guo X.J., Zou S.Y., Yu H.Y., Liu Z.W., Zhang Y.F., Wang K.X. Improving soft magnetic properties of Mn-Zn ferrite by rare earth ions doping. *AIP Adv.* 2018. V. 8. 047807. DOI: 10.1063/1.4993645.
12. Nikumbh A.K., Pawar R.A., Nighot D.V., Gugale G.S., Sangale M.D., Khanvilkar M.B., Nagawade A.V. Structural, electrical, magnetic and dielectric properties of rare-earth substituted cobalt ferrites nanoparticles synthesized by the co-precipitation method. *Magn. Magn. Mater.* 2014. V. 355. P. 201–209. DOI: 10.1016/j.jmmm.2013.11.052.
13. Li L., Jiang J., Xu F. Synthesis and ferrimagnetic properties of novel Sm-substituted LiNi ferrite-polyaniline nanocomposite. *Mater. Lett.* 2007. V. 61. P. 1091-1096. DOI: 10.1016/j.matlet.2006.06.061.
14. Abdel Maksoud M.I.A., El-Ghandour A., Ashour A.H., Atta M.M., Abdelhaleem S., El-Hanbaly A.H., Fahim R.A., Kassem S.M., Shalaby M.S., Awed A.S. La³⁺ doped $\text{LiCo}_{0.25}\text{Zn}_{0.25}\text{Fe}_2\text{O}_4$ spinel ferrite nanocrystals: Insights on structural, optical and magnetic properties. *J. Rare Earths.* 2021. V. 39. P. 75-82. DOI: 10.1016/j.jre.2019.12.017.
15. Mahmoudi M., Kavanlouei M., Maleki-Ghaleh H. Effect of composition on structural and magnetic properties of nanocrystalline ferrite $\text{Li}_{0.5}\text{Sm}_x\text{Fe}_{2.5-x}\text{O}_4$. *Powder Metall. Met. Ceram.* 2015. V. 54(1-2) P. 31-39. DOI: 10.1007/s11106-015-9676-9.
16. Inbanathan S.S.R., Vaithyanathan V., Arout Chelvane J., Markandeyulu G., Kamala Bharathi K. Mössbauer studies and enhanced electrical properties of R (R=Sm, Gd and Dy) doped Ni ferrite. *Magn. Magn. Mater.* 2014. V. 353. P. 41-46. DOI: 10.1016/j.jmmm.2013.10.019.
17. Gajula G.R., Buddiga L.R. Structural, ferroelectric, dielectric, impedance and magnetic properties of Gd and Nb doped barium titanate-lithium ferrite solid solutions. *Magn. Magn. Mater.* 2020. V. 494. 165822. DOI: 10.1016/j.jmmm.2019.165822.
18. Ashour A.H., Hemeda O.M., Heiba Z.K., Al-Zahrani S.M. Electrical and thermal behavior of PS/ferrite composite. *Magn. Magn. Mater.* 2014. V. 369. P. 260-267. DOI: 10.1016/j.jmmm.2014.06.005.
19. Abdellatif M.H., El-Komy G.M., Azab A.A. Magnetic characterization of rare earth doped spinel ferrite. *Magn. Magn. Mater.* 2017. V. 442. P. 445-452. DOI: 10.1016/j.jmmm.2017.07.020.
8. Isaev I.M., Kostishin V.G., Korovushkin V.V., Shipko M.N., Timofeev A.V., Mironovich A.Yu., Salogub D.V., Shakirzyanov R.I. Crystal chemistry and magnetic properties of polycrystalline spinel ferrites $\text{Li}_{0.33}\text{Fe}_{2.29}\text{Zn}_{0.21}\text{Mn}_{0.17}\text{O}_4$. *Zhurn. Neorgan. Khim.* 2021. V. 66. N 12. P. 1792-1800 (in Russian). DOI: 10.31857/S0044457X21120059.
9. Isaev I.M., Kostishin V.G., Korovushkin V.V., Salogub D.V., Shakirzyanov R.I., Timofeev A.V., Mironovich A.Yu. Magnetic and radio absorbing properties of polycrystalline ferrite-spinel $\text{Li}_{0.33}\text{Fe}_{2.29}\text{Zn}_{0.21}\text{Mn}_{0.17}\text{O}_4$. *Zhurn. Tekhn. Fiziki.* 2021. V. 91. N 9. P. 1376-1380 (in Russian). DOI: 10.21883/JTF.2021.09.51217.74-21.
10. AsifIqbal M., Islam M.U., Ali I., Khan M.A., Sadiq I., Ali I. High frequency dielectric properties of Eu+3-substituted Li-Mg ferrites synthesized by sol-gel auto-combustion method. *J. Alloys Compd.* 2014. V. 586. P. 404-410. DOI: 10.1016/j.jallcom.2013.10.066.
11. Zhong X.C., Guo X.J., Zou S.Y., Yu H.Y., Liu Z.W., Zhang Y.F., Wang K.X. Improving soft magnetic properties of Mn-Zn ferrite by rare earth ions doping. *AIP Adv.* 2018. V. 8. 047807. DOI: 10.1063/1.4993645.
12. Nikumbh A.K., Pawar R.A., Nighot D.V., Gugale G.S., Sangale M.D., Khanvilkar M.B., Nagawade A.V. Structural, electrical, magnetic and dielectric properties of rare-earth substituted cobalt ferrites nanoparticles synthesized by the co-precipitation method. *Magn. Magn. Mater.* 2014. V. 355. P. 201–209. DOI: 10.1016/j.jmmm.2013.11.052.
13. Li L., Jiang J., Xu F. Synthesis and ferrimagnetic properties of novel Sm-substituted LiNi ferrite-polyaniline nanocomposite. *Mater. Lett.* 2007. V. 61. P. 1091-1096. DOI: 10.1016/j.matlet.2006.06.061.
14. Abdel Maksoud M.I.A., El-Ghandour A., Ashour A.H., Atta M.M., Abdelhaleem S., El-Hanbaly A.H., Fahim R.A., Kassem S.M., Shalaby M.S., Awed A.S. La³⁺ doped $\text{LiCo}_{0.25}\text{Zn}_{0.25}\text{Fe}_2\text{O}_4$ spinel ferrite nanocrystals: Insights on structural, optical and magnetic properties. *J. Rare Earths.* 2021. V. 39. P. 75-82. DOI: 10.1016/j.jre.2019.12.017.
15. Mahmoudi M., Kavanlouei M., Maleki-Ghaleh H. Effect of composition on structural and magnetic properties of nanocrystalline ferrite $\text{Li}_{0.5}\text{Sm}_x\text{Fe}_{2.5-x}\text{O}_4$. *Powder Metall. Met. Ceram.* 2015. V. 54(1-2) P. 31-39. DOI: 10.1007/s11106-015-9676-9.
16. Inbanathan S.S.R., Vaithyanathan V., Arout Chelvane J., Markandeyulu G., Kamala Bharathi K. Mössbauer studies and enhanced electrical properties of R (R=Sm, Gd and Dy) doped Ni ferrite. *Magn. Magn. Mater.* 2014. V. 353. P. 41-46. DOI: 10.1016/j.jmmm.2013.10.019.
17. Gajula G.R., Buddiga L.R. Structural, ferroelectric, dielectric, impedance and magnetic properties of Gd and Nb doped barium titanate-lithium ferrite solid solutions. *Magn. Magn. Mater.* 2020. V. 494. 165822. DOI: 10.1016/j.jmmm.2019.165822.
18. Ashour A.H., Hemeda O.M., Heiba Z.K., Al-Zahrani S.M. Electrical and thermal behavior of PS/ferrite composite. *Magn. Magn. Mater.* 2014. V. 369. P. 260-267. DOI: 10.1016/j.jmmm.2014.06.005.
19. Abdellatif M.H., El-Komy G.M., Azab A.A. Magnetic characterization of rare earth doped spinel ferrite. *Magn. Magn. Mater.* 2017. V. 442. P. 445-452. DOI: 10.1016/j.jmmm.2017.07.020.

20. **Bulai G., Diamandescu L., Dumitru I., Gurlui S., Feder M., Caltun O.F.** Effect of rare earth substitution in cobalt ferrite bulk materials. *Magn. Magn. Mater.* 2015. V. 390. P. 123-131. DOI: 10.1016/j.jmmm.2015.04.089.
21. **Rady K.E., Shams M.S.** Study the effect of Gd³⁺ incorporation into nanocrystalline (Ni-Ti) substituted Mn-Zn ferrites on its structure and functional properties. *Magn. Magn. Mater.* 2017. V. 426. P. 615-620. DOI: 10.1016/j.jmmm.2016.10.160.
22. **Lysenko E.N., Vlasov V.A., Nikolaeva S.A., Nikolaev E.V.** TG, DSC, XRD, and SEM studies of the substituted lithium ferrite formation from milled Sm₂O₃/Fe₂O₃/Li₂CO₃ precursors. *J. Therm. Anal. Calorim.* 2023. V. 148. P. 1445-1453. DOI: 10.1007/s10973-022-11665-1.
23. **Рогачев А.С.** Механическая активация гетерогенных экзотермических реакций в порошковых смесях. *Усп. химии.* 2019. Т. 88. № 9. С.875-900. DOI: 10.1070/RCR4884.
24. **Стрелецкий А.Н., Воробьева Г.А., Колбанев И.В., Леонов А.В., Кириленко В.Г., Гришин Л.И., Долгобородов А.Ю.** Механохимия Bi₂O₃. 2. Механическая активация и термические реакции в энергонасыщенной системе Al+Bi₂O₃. *Коллоид. журн.* 2019. Т. 81. № 5. С.625-633. DOI: 10.1134/S002329121905015X.
25. **Sarkar K., Mondal R., Dey S., Majumder S., Kumar S.** Presence of mixed magnetic phase in mechanically milled Co_{0.5}Zn_{0.5}Fe₂O₄: A study on structural, magnetic and hyperfine properties. *Magn. Magn. Mater.* 2019. V. 487. 165303. DOI: 10.1016/j.jmmm.2019.165303.
26. **Nili-Ahmababdi M., Sarraf-Mamoory R., Yourdkhani A., Diaconu A., Rotaru A.** Magnetic and electrical properties of Mg_{1-x}CoxFe₂O₄ (x=0-0.15) ceramics prepared by the solid-state method. *J. Eur. Ceram. Soc.* 2021. V. 42. P. 442-447. DOI: 10.1016/j.eurceramsoc.2021.10.046.
27. **Lysenko E.N., Nikolaev E.V., Surzhikov A.P., Nikolaeva S.A., Plotnikova I.V.** The influence of reagents ball milling on the lithium ferrite formation. *J. Therm. Anal. Calorim.* 2019. V. 138. P. 2005-2013. DOI: 10.1007/s10973-019-08334-1.
28. **Lysenko E.N., Surzhikov A.P., Vlasov V.A., Malyshev A.V., Nikolaev E.V.** Thermal analysis study of solid-phase synthesis of zinc- and titanium-substituted lithium ferrites from mechanically activated reagents. *J. Therm. Anal. Calorim.* 2015. V. 122. P. 1347-1353. DOI: 10.1007/s10973-015-4849-9.
29. **Kessler M., Rinaldi R.** Kinetic Energy Dose as a Unified Metric for Comparing Ball Mills in the Mechanocatalytic Depolymerization of Lignocellulose. *Front. Chem.* 2022. V. 9. 816553. DOI: 10.3389/fchem.2021.816553.
30. **Kessler M., Woodward R.T., Wong N., Rinaldi R.** Kinematic Modeling of Mechanocatalytic Depolymerization of α -Cellulose and Beechwood. *Chem. Sus. Chem.* 2018. V. 11. P. 552 – 561. DOI: 10.1002/cssc.201702060.
31. **Lysenko E.N., Surzhikov A.P., Astafyev A.L.** Thermomagnetometric analysis of lithium ferrites. *J. Therm. Anal. Calorim.* 2019. V. 136. P. 441-445. DOI: 10.1007/s10973-018-7678-9.
32. **Yousefi T., Mostaedi M.T., Ghasemi M., Ghadirifar A.** A Simple Way to Synthesize of Samarium Oxide Nanoparticles: Characterization and Effect of pH on Morphology. *Synth. React. Inorg. Met.-Org. Nano-Met. Chem.* 2016. V. 46. P. 137-142. DOI: 10.1080/15533174.2014.900795.
20. **Bulai G., Diamandescu L., Dumitru I., Gurlui S., Feder M., Caltun O.F.** Effect of rare earth substitution in cobalt ferrite bulk materials. *Magn. Magn. Mater.* 2015. V. 390. P. 123-131. DOI: 10.1016/j.jmmm.2015.04.089.
21. **Rady K.E., Shams M.S.** Study the effect of Gd³⁺ incorporation into nanocrystalline (Ni-Ti) substituted Mn-Zn ferrites on its structure and functional properties. *Magn. Magn. Mater.* 2017. V. 426. P. 615-620. DOI: 10.1016/j.jmmm.2016.10.160.
22. **Lysenko E.N., Vlasov V.A., Nikolaeva S.A., Nikolaev E.V.** TG, DSC, XRD, and SEM studies of the substituted lithium ferrite formation from milled Sm₂O₃/Fe₂O₃/Li₂CO₃ precursors. *J. Therm. Anal. Calorim.* 2023. V. 148. P. 1445-1453. DOI: 10.1007/s10973-022-11665-1.
23. **Rogachev A.** Mechanical activation of heterogeneous exothermic reactions in powder mixtures. *Usp. Khim.* 2019. V. 88. N 9. P. 875 (in Russian). DOI: 10.1070/RCR4884.
24. **Streletskaia A.N., Vorob'eva G.A., Kolbanov I.V., Leonov A.V., Kirilenko V.G., Grishin L.I., Dolgorodov A.Yu.** Mechanochemistry of Bi₂O₃. 2. Mechanical activation and thermal reactions in a high-energy Al+Bi₂O₃ system. *Colloid J.* 2019. V. 81. P. 575-582. DOI: 10.1134/S1061933X19050156.
25. **Sarkar K., Mondal R., Dey S., Majumder S., Kumar S.** Presence of mixed magnetic phase in mechanically milled Co_{0.5}Zn_{0.5}Fe₂O₄: A study on structural, magnetic and hyperfine properties. *Magn. Magn. Mater.* 2019. V. 487. 165303. DOI: 10.1016/j.jmmm.2019.165303.
26. **Nili-Ahmababdi M., Sarraf-Mamoory R., Yourdkhani A., Diaconu A., Rotaru A.** Magnetic and electrical properties of Mg_{1-x}CoxFe₂O₄ (x = 0-0.15) ceramics prepared by the solid-state method. *J. Eur. Ceram. Soc.* 2021. V. 42. P. 442-447. DOI: 10.1016/j.eurceramsoc.2021.10.046.
27. **Lysenko E.N., Nikolaev E.V., Surzhikov A.P., Nikolaeva S.A., Plotnikova I.V.** The influence of reagents ball milling on the lithium ferrite formation. *J. Therm. Anal. Calorim.* 2019. V. 138. P. 2005-2013. DOI: 10.1007/s10973-019-08334-1.
28. **Lysenko E.N., Surzhikov A.P., Vlasov V.A., Malyshev A.V., Nikolaev E.V.** Thermal analysis study of solid-phase synthesis of zinc- and titanium-substituted lithium ferrites from mechanically activated reagents. *J. Therm. Anal. Calorim.* 2015. V. 122. P. 1347-1353. DOI: 10.1007/s10973-015-4849-9.
29. **Kessler M., Rinaldi R.** Kinetic Energy Dose as a Unified Metric for Comparing Ball Mills in the Mechanocatalytic Depolymerization of Lignocellulose. *Front. Chem.* 2022. V. 9. 816553. DOI: 10.3389/fchem.2021.816553.
30. **Kessler M., Woodward R.T., Wong N., Rinaldi R.** Kinematic Modeling of Mechanocatalytic Depolymerization of α -Cellulose and Beechwood. *Chem. Sus. Chem.* 2018. V. 11. P. 552 – 561. DOI: 10.1002/cssc.201702060.
31. **Lysenko E.N., Surzhikov A.P., Astafyev A.L.** Thermomagnetometric analysis of lithium ferrites. *J. Therm. Anal. Calorim.* 2019. V. 136. P. 441-445. DOI: 10.1007/s10973-018-7678-9.
32. **Yousefi T., Mostaedi M.T., Ghasemi M., Ghadirifar A.** A Simple Way to Synthesize of Samarium Oxide Nanoparticles: Characterization and Effect of pH on Morphology. *Synth. React. Inorg. Met.-Org. Nano-Met. Chem.* 2016. V. 46. P. 137-142. DOI: 10.1080/15533174.2014.900795.

33. Lysenko E.N., Nikolaev E.V., Vasendina E.A. Investigation of heating rate effect on solid-phase interaction in Li_2CO_3 - Fe_2O_3 reaction mixture. *IOP Conf. Ser.: Mater. Sci. Eng.* 2015. V. 81. 012104. DOI: 10.1088/1757-899X/81/1/012104.
34. Lysenko E.N., Malyshev A.V., Vlasov V.A., Nikolaev E.V., Surzhikov A.P. Microstructure and thermal analysis of lithium ferrite pre-milled in a high-energy ball mill. *J. Therm. Anal. Calorim.* 2018. V. 134. P. 127-133. DOI: 10.1007/s10973-018-7549-4.
35. Левин Б.Е., Третьяков Ю.Д., Летюк Л.М. Физико-химические основы получения, свойства и применение ферритов. М.: Металлургия. 1979. 471 с.
36. Teixeira Soreto S., Graça M.P.F., Costa L.C., Valente M.A. Study of the influence of thermal treatment on the magnetic properties of lithium ferrite prepared by wet ball-milling using nitrates as raw material. *Mater. Sci. Eng. B*. 2014. V. 186. P. 83–88. DOI: 10.1016/j.mseb.2014.03.008.
37. Verma V., Pandey V., Singh S., Aloysius R.P., Anna-poorani S., Kotanala R.K. Comparative study of structural and magnetic properties of nano-crystalline $\text{Li}_{0.5}\text{Fe}_{2.5}\text{O}_4$ prepared by various methods. *Physica B*. 2009. V. 404. P. 2309-2314. DOI: 10.1016/j.physb.2009.04.034.
38. Ahniyaz A., Fujiwara T., Song S.-W., Yoshimura M. Low temperature preparation of α - LiFe_5O_8 fine particles by hydrothermal ball milling. *Solid State Ionics*. 2002. V. 151. P. 419-423. DOI: 10.1016/S0167-2738(02)00548-9.
33. Lysenko E.N., Nikolaev E.V., Vasendina E.A. Investigation of heating rate effect on solid-phase interaction in Li_2CO_3 - Fe_2O_3 reaction mixture. *IOP Conf. Ser.: Mater. Sci. Eng.* 2015. V. 81. 012104. DOI: 10.1088/1757-899X/81/1/012104.
34. Lysenko E.N., Malyshev A.V., Vlasov V.A., Nikolaev E.V., Surzhikov A.P. Microstructure and thermal analysis of lithium ferrite pre-milled in a high-energy ball mill. *J. Therm. Anal. Calorim.* 2018. V. 134. P. 127-133. DOI: 10.1007/s10973-018-7549-4.
35. Levin B.E., Tretyakov Yu.D., Letyuk L.M. Physical and chemical bases of obtaining, properties and application of ferrites. M.: Metallurgiya. 1979. 471 p. (in Russian).
36. Teixeira Soreto S., Graça M.P.F., Costa L.C., Valente M.A. Study of the influence of thermal treatment on the magnetic properties of lithium ferrite prepared by wet ball-milling using nitrates as raw material. *Mater. Sci. Eng. B*. 2014. V. 186. P. 83–88. DOI: 10.1016/j.mseb.2014.03.008.
37. Verma V., Pandey V., Singh S., Aloysius R.P., Anna-poorani S., Kotanala R.K. Comparative study of structural and magnetic properties of nano-crystalline $\text{Li}_{0.5}\text{Fe}_{2.5}\text{O}_4$ prepared by various methods. *Physica B*. 2009. V. 404. P. 2309-2314. DOI: 10.1016/j.physb.2009.04.034.
38. Ahniyaz A., Fujiwara T., Song S.-W., Yoshimura M. Low temperature preparation of α - LiFe_5O_8 fine particles by hydrothermal ball milling. *Solid State Ionics*. 2002. V. 151. P. 419-423. DOI: 10.1016/S0167-2738(02)00548-9.

Поступила в редакцию 04.07.2023
Принята к опубликованию 09.11.2023

Received 04.07.2023
Accepted 09.11.2023